MYB5-like and bHLH influence flavonoid composition in pomegranate

Plant Science

Arlotta, Carmen; Puglia, Giuseppe D.; Genovese, Claudia; Toscano, Valeria; Karlova, R.B. et al

https://doi.org/10.1016/j.plantsci.2020.110563

Plant Science 298 (2020) 110563

Contents lists available at ScienceDirect

Plant Science

journal homepage: www.elsevier.com/locate/plantsci

Research Article

MYB5-like and bHLH influence flavonoid composition in pomegranate

Carmen Arlotta[a], Giuseppe D. Puglia[a,*], Claudia Genovese[a], Valeria Toscano[a], Rumyana Karlova[b], Jules Beekwilder[b], Ric C.H. De Vos[b], Salvatore A. Raccuia[a]

[a] Consiglio Nazionale delle Ricerche, Istituto per i Sistemi Agricoli e Forestali del Mediterraneo (CNR-ISAFOM) U.O.S. Catania, Via Empedocle, 58, 95128, Catania, Italy
[b] Wageningen Plant Research, Bioscience, 6700 AA, Wageningen, the Netherlands

ARTICLE INFO

Keywords:
Punica granatum
Polyphenolic compounds
Transcription factors
Metabolomics
Nicotiana benthamiana
Flavonoid pathway genes

ABSTRACT

The fruit of the pomegranate (*Punica granatum* L.) is an important nutraceutical food rich in polyphenolic compounds, including hydrolysable tannins, anthocyanins and flavonols. Their composition varies according to cultivar, tissue and fruit development stage and is probably regulated by a combination of MYB and bHLH type transcription factors (TFs). In this study, metabolomics analysis during fruit developmental stages in the main pomegranate cultivars, Wonderful and Valenciana with contrasting colour of their ripe fruits, showed that flavonols were mostly present in flowers while catechins were highest in unripe fruits and anthocyanins in late fruit maturation stages. A novel MYB TF, *PgMYB5-like*, was identified, which differs from previously isolated pomegranate TFs by unique C-terminal protein motifs and lack of the amino-acid residues conserved among anthocyanins promoting MYBs. In both pomegranate cultivars the expression of *PgMYB5-like* was high at flowering stage, while it decreased during fruit ripening. A previously identified bHLH-type TF, *PgbHLH*, also showed high transcript levels at flowering stage in both cultivars, while it showed a decrease in expression during fruit ripening in cv. Valenciana, but not in cv. Wonderful. Functional analysis of both TFs was performed by agro-infiltration into *Nicotiana benthamiana* leaves. Plants infiltrated with the *PgMYB5-like* + *PgbHLH* combined construct showed a specific and significant accumulation of intermediates of the flavonoid pathway, especially dihydroflavonols, while anthocyanins were not produced. Thus, we propose a role for *PgMYB5-like* and *PgbHLH* in the first steps of flavonoid production in flowers and in unripe fruits. The expression patterns of these two TFs may be key in determining the differential flavonoid composition in both flowers and fruits of the pomegranate varieties Wonderful and Valenciana.

1. Introduction

Pomegranate is a rich source of potentially nutraceutical active compounds including organic acids, vitamins and phenols [1,2] with antioxidant and antiproliferative properties on cancer cells [3–5]. Three classes of polyphenolic compounds have been studied as potential bioactive ingredients: the hydrolysable tannins, the anthocyanins and the flavonols. A number of recent studies have described metabolic profiles in different pomegranate cultivars, in particular at the commercially relevant mature fruit stage [6,7]. Only limited information is available on the concentrations of these compounds in different tissues and developmental stages of the pomegranate. To address the relationship between metabolite composition and genetic factors involved in their biosynthesis, such information can be very valuable. Biosynthesis of flavonoids is widespread in the plant kingdom [8]. It includes several branches of a common pathway, which can lead to flavonols, but also to flavan-3-ols and anthocyanins [9]. Anthocyanins are responsible of tissue pigmentation. The flavan-3-ols can be found in monomeric form, called catechins with a radical-scavenging activity [10,11], or in polymeric form, such as proanthocyanidins which protect plants from biotic and abiotic stressors [12]. Flavonols are often suggested to be involved in the protection of plant cells from UV and oxygen radical damage [13–15]. In the last decade, the beneficial role of flavonoids for human health has been well-documented, in particular their hepatoprotective, antibacterial, anti-inflammatory anti-oxidant and anticancer activity [16–18].

The biosynthesis of flavonoids in pomegranate has been studied in different tissues, and a number of genes have been identified [19–23]. The main biosynthetic structural flavonoid pathway genes include chalcone synthase (CHS), which is the first committed enzyme in the pathway, flavonoid 3'-hydroxylase (F3'H) and flavonoid 3',5'-hydroxylase (F3'5'H), which are both P450 enzymes that catalyse the hydroxylation of dihydrokaempferol to form dihydroquercetin and dihydromyricetin respectively [24], dihydroflavonols 4-reductase (DFR),

* Corresponding author.
E-mail address: giuseppediego.puglia@cnr.it (G.D. Puglia).

https://doi.org/10.1016/j.plantsci.2020.110563
Received 5 March 2020; Received in revised form 25 May 2020; Accepted 11 June 2020
Available online 20 June 2020
0168-9452/

that reduces dihydroflavonols to corresponding colourless leucoanthocyanidins [25] and UDP-glucose: flavonoid 3-O-glucosyltransferase (UFGT), which couple sugar molecules to anthocyanidin aglycons [26]. Regulation of the flavonoid pathway in pomegranate involves a combination of transcription factors (TFs) from the WD40, MYB and bHLH classes [27–29]. The activity of the pomegranate regulatory gene *PgWD40* was demonstrated in an Arabidopsis *ttg1-9* mutant and was shown to be dependent on MYB function [30]. The interaction between MYB and bHLH is carried out through a conserved amino acid signature with [D/E]L × 2[R/K] × 3 L × 6 L × 3R present in the R2R3 MYB domain [31]. On the basis of these conserved amino-acid sequence motifs present carboxy-terminal of the MYB domain, the R2R3-type MYB factors have been categorised into 24 subgroups (SG) [32]. This characterization showed the presence of functional subgroups among Arabidopsis MYB TFs [32,33] including: the *AtMYB3* and *AtMYB4* (SG 4) encoding for transcriptional repressors [34]; the *AtMYB123/TT2* (SG 5) which is involved in the synthesis proanthocyanidins [35]; the *AtMYB75/PAP1*, *AtMYB90/PAP2* and *AtMYB113* (SG 6) that control the synthesis of anthocyanins [36,37]; the *AtMYB11*, *AtMYB12* and *AtMYB111* (SG 7) that regulate the synthesis of flavonols [38]; the *AtMYB0/GL1*, *AtMYB23* and *AtMYB66/WER* (SG 15) that control trichome development [39]. The MYB-bHLH network regulation was studied in *Petunia hybrida*, *Antirrhinum majus* and *Zea mays* as regulators of anthocyanin biosynthesis and in *A. thaliana* as regulator of anthocyanin and proanthocyanin biosynthesis [40,41]. Using transient expression, TFs *ROS1* (MYB type) and *DEL* (bHLH type) from *A. majus* were shown to induce anthocyanin production in tomato [42] and in *Nicotiana benthamiana,* which is widely used for heterologous expression [43,44]. In *N. benthamiana*, the expression of both *ROS1* and *DEL* induced a single anthocyanin production (delphinidin-3-rutinoside) [45]. However, for pomegranate TFs, only limited information is available on the bHLH-MYB interaction and the effects of their overexpression on phenolic metabolite content.

In this study, the metabolic profiles of two pomegranate cultivars differing in fruit colour were compared during fruit development, in association with expression profiles of the flavonoid pathway genes and uncharacterized pomegranate MYB and bHLH genes.

2. Materials and methods

2.1. Plant material

From June to October, leaves, flowers and fruits at different development stages were harvested from Valenciana (a rose-coloured fruit cultivar) and Wonderful (a red-coloured fruit cultivar) *P. granatum* trees. The two cultivars, belonging to a germplasm collection of CNR-ISAFOM of Catania (Italy), were grown under the same environmental conditions with the same applied agronomic practices in a randomized block field. We collected flowers, three fruit developmental stages including unripe fruit, turning fruit and ripe fruit, and during the last sampling (October) mature leaves were also collected (Fig. 1). We sampled 3 trees per cultivar and for each tree we collected and pooled 3 leaves, flowers or fruits (i.e. each tree is a biological repeat). During each sampling time the arils were separated from the rest of the fruit tissues and, as for flowers and leaves, immediately immersed in liquid nitrogen. Leaves and flowers were ground to a fine powder with liquid nitrogen, while arils were treated in two different ways: 1) Unripe, Turning and Ripe arils were ground as a whole (flesh plus seed, F + S); 2) for both Turning and Ripe arils the frozen flesh (F) part of the aril was also firstly separated from the seed and then ground; for unripe fruit the aril flesh could not be separated from the seed. The obtained powders were used for metabolomics analyses and RNA extractions.

2.2. Metabolite extraction and LC-PDA-MS analysis

From each sample 300 mg of frozen powder was extracted with 900 µL of methanol containing 5 % formic acid (FA). The extracts were sonicated for 15 min, centrifuged at max speed for 15 min and filtered (0.45 µm). Metabolite analysis was carried out using an Acquity UPLC system (Waters, MA, USA) equipped with a photodiode array detector (PDA) and coupled to an LTQ-Orbitrap FTMS hybrid Mass Spectrometer (Thermo Scientific, MA, USA). Separation was performed on a Luna C18-reversed phase column (150 × 2 mm, 3 µm; Phenomenex, CA, USA). Ultrapure water with 0.1 % formic acid (eluent A) and acetonitrile acidified with 0.1 % formic acid (eluent B) were used as mobile phase with a linear gradient from 5 to 35 % eluent B at a flow rate of 0.19 mL/min for 45 min, following by washing and stabilization. A mass resolution of 60,000 HWHM was employed for data acquisition. Samples were analysed using a mass range of *m/z* 150–2000, in negative ionization mode. Identification of detected metabolites was based on their retention time, accurate masses of both the parent and fragment ions, in combination with their PDA absorbance spectra (recorded at 240–600 nm). The acquired LC-PDA-MS data were analysed using Xcalibur 2.1 software (Thermo Scientific, MA, USA). As was determined by analysis of authentic standards, it appeared that in our LCMS setup the anthocyanins were most sensitively detected as their [M + H2O-H]- adduct, rather than their molecular ion; for the large gallotannins their double charged molecular ions [M − H]2- were the most prominent in the mass spectra (cf. Sun et al. [46]). These most abundant ions, rather than their molecular ions, were therefore selected for peak area integration by the QualBrowser module within Xcalibur.

2.3. Pomegranate regulatory complex genes isolation

To characterize *PgPAP-like*, *PgMYB5-like*, *PgMYB4-like* and *PgbHLH* transcript sequences, total RNA was extracted as from leaves of cultivar Wonderful as described by Zarei et al. [47]. The extracts were analysed with QIAxcel instrument by the mean of capillary electrophoresis, that provides a RNA Integrity Score (RIS) as function of the ratio of 18S and 28S rRNA peaks. One µg of total RNA extracted from different analysed tissues was used to synthesize first–strand cDNA using Superscript II Reverse transcriptase (Invitrogen, Italy) with oligo (dT) in 20 µL total volume. To isolate flavonoid pomegranate regulatory complex genes, specific oligomeric primers were designed basing on the DNA sequences of *P. granatum* L. available in the literature and in the National Centre for Biotechnology Information (NCBI) Nucleotide database (Table 1). CDS amplifications were cloned into the pCR8/GW/TOPO-TA vector (Invitrogen, Thermo Fisher Scientific) and verified by DNA sequencing. Predicted introns were removed *in silico* and obtained splices were used for sequences alignments using Clustal Omega [48], while Mega 7 software [49] was used to construct phylogenetic trees with Neighbour-Joining clustering method. The sequences motif discovery was carried out using MEME suite 5.0.5 [50]. The cDNA sequences of *PgPAP-like*, *PgMYB5-like* and *PgMYB4-like* were deposited to GenBank database (GenBank accession numbers from MT495437 to MT495439).

2.4. Quantitative PCR assays

Total RNA was extracted from leaves, flowers and two aril developmental stages (Unripe F + S and Ripe F + S) of both Valenciana and Wonderful cultivars, as described above. qPCR primers were designed with Primer3 [51] using the CDS sequences of *PgPAP-like*, *PgMYB5-like*, *PgMYB4-like* and *PgbHLH*, while for *PgCHS, PgF*3'5'*H, PgDFR* and *PgUFGT* the relative sequences available at NCBI Nucleotide database were used. The *PgRPSII* (Ribosomial Protein S) was utilized as housekeeping gene using primers from a previous study on pomegranate [52] (Table 2). For all qPCR primers amplicon length of 90–150 bp and 59 − 64 °C of melting temperature range were selected as designing parameter.

The RT–qPCRs were carried out using as template the cDNA libraries obtained separately from leaf, flower, unripe aril (F + S), and ripe aril (F + S) from Valenciana and Wonderful, for each tissue three

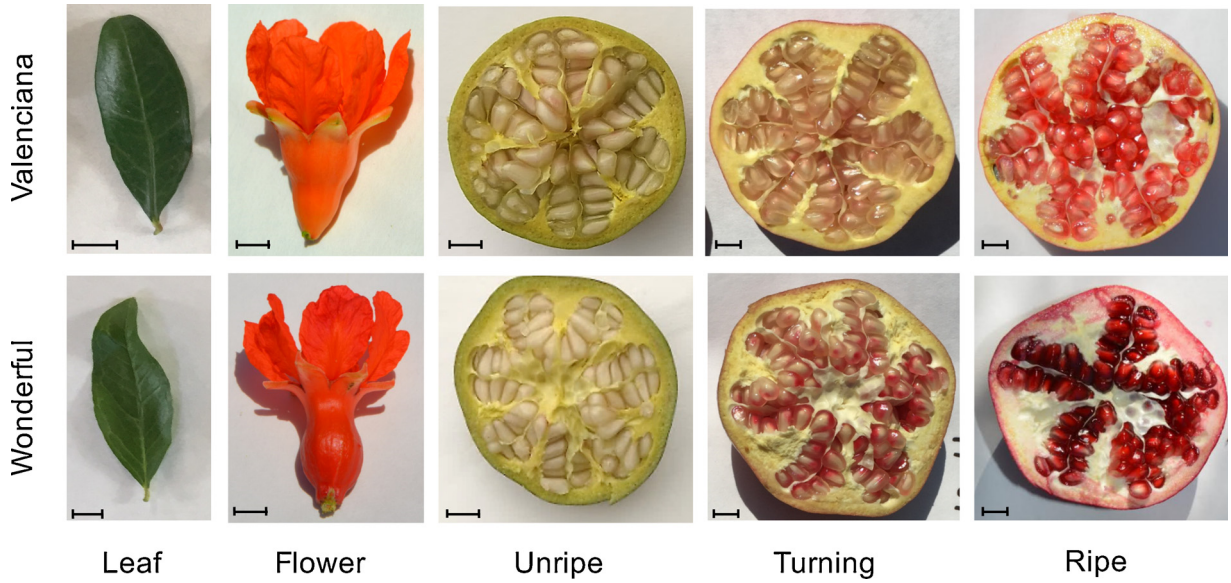

Fig. 1. Sampled tissues: mature leaf, flower and three fruit development stages of "Valenciana" and "Wonderful" pomegranates cultivars.

independent biological replicates and three technical replicates of each biological were used. The reactions were performed on a Rotor Gene-6000 (Qiagen, Hilden, Germany) with the following condition: first step at 95 °C for 2 min and afterwards 40 cycles alternating between 95 °C for 5 s and 60 °C for 10 s. Each 20 µL reaction mixture consisted of: 10 µL of 2x QuantiNova™ SYBR® Green PCR Master Mix (Qiagen, Hilden, Germany), 1.4 µL each of forward and reverse primer (10 µM), and 1 µL of cDNA (80 ng). The melting curves were assessed for the different primers couples. The Take Off Point (TOP) and the amplification value of the primers were obtained automatically by the Rotor-Gene system selecting the "comparative quantitation analysis of cycling" method. These values were used to calculate the relative expression ratio by the Pfaffl method [53]. The expression levels were compared with the *PgRPSII* housekeeping gene and the unripe aril F + S of Valenciana was considered as calibrator tissue and set to value of 1.

2.5. Agroinfiltration

Nicotiana benthamiana infiltrations were carried out using isolated CDS as described previously [54,55]. *Agrobacterium tumefaciens*, AGL0 strain [56], and cDNA-constructs (pBIN, 35S-*PgMYB5-like* and/or 35S-*PgbHLH*, 35S-ROS1 and 35S-DEL) were mixed in equal volumes. The plants were grown in a greenhouse with 16 h light at 28 °C and 3 mL of strain mixtures were infiltrated into the abaxial side of leaves of two-week-old plants using a syringe. Six *N. benthamiana* plants per construct were used and two leaves per plants were agroinfiltrated. The first three plants per construct were harvested four days after agroinfiltration, the other three plants six days after agroinfiltration. For each harvested sample we performed an individual metabolite extraction and LC-PDA-Orbitrap FTMS analysis as described above. Here an essentially untargeted analysis was carried out as described by De Vos et al. [57], using the MetAlign software package [58] for baseline correction, noise estimation and mass peak alignment, with a detection threshold of 10,000 ions per scan. MSClust software [59] was used to cluster mass peaks originating from the same metabolite, including adducts, fragments and isotopes, so to reconstruct in-source mass spectra and obtain a single total ion intensity value per compound. Zero values for compound intensity in samples, *i.e.* none of the signals of that compound was above the detection threshold.

2.6. Statistical analyses

Principal Component Analysis (PCA) was performed for metabolomics data from the various pomegranate tissues and from the *N. benthamiana* infiltrated leaves, using SIMCA tool version 14 (MKS Umetrics AB, 1992–2015), after log-transformation and normalization (Pareto scaling) across samples. The relative intensity levels of compounds resulting from the MSClust software were plotted as heat maps across different tissues using R (R Core Team 2018) and significantly differing compounds ($p \leq 0.05$) were identified through Student's *t*-test. Gene expression levels variance was assessed through one-way ANOVA with Student-Newman-Keuls means test using CoSTAT software (CoHort software, Monterey, CA, USA) comparing the variance among all samples or among tissues of each genotype. Correlation of structural and regulatory genes of flavonoid biosynthesis pathway with flavonoids or anthocyanins content was assessed with Pearson correlation test using CoSTAT software (CoHort software, Monterey, CA, USA) and a p value ≤ 0.05 was regarded as being significant and was reported in the text only when it was specifically lower then this threshold and key to the conclusion.

Table 1
Cloning primers designed to isolate complete CDS. *Ta* PCR annealing temperature.

Gene name	Primer sequence (5'-3')	Ta °C	Product size (bp)	Accession number
PgPAP-like	F: ATGGAGGAAGCTGCTTCTTTTCGAAGAGTAAGG R: TTATATTATCCCCATCTCTTCTTGGTCGGCACATAG	56	1364	KP726347.1
PgMYB5-like	F: ATGACGGCACCAACAAGGCG R: TTAAAATCGCTTATCAGCGGTCAACATGTCCTC	56	1136	HM056531.1
PgMYB4-like	F: ATGGGAAGGTCTCCTTGCTGTGAGAAAG R: TCATTTCATCTCCAAACTTCTGTAATCCAATACGCC	56	899	KM881712.1
PgbHLH	F: ATGGCTGTGCCGCCCAGTAG R: CTAAGAGTCAGTGTGGGGTATAAGCTGTTGG	56	2070	KF874658.1

Table 2
qPCR primers designed based on obtained sequences contigs and sequences from NCBI database. *Ta* PCR annealing temperature.

Gene name	Primer sequence (5'-3')	GC %	Ta °C	Product size (bp)	Accession number
PgCHS	F: CGCTAGGCAGGACATTGTGG	60	58	101	KF841615.2
	R: GGGTGATCTTCGACTTGGGC	60			
PgF3'5'H	F: GGCACTCCTTTTGGTATGTCC	52	58	101	KU058892.1
	R: TGTCGAGGACCTGATTACGC	55			
PgDFR	F: CACAGAGAAGGTGTCGTTCTC	52	58	118	KF841618.1
	R: GAGAAGCCCCTTCTCCCTG	63			
PgUFGT	F: GGCCGATCATTCCCACGAGCA	62	58	130	KF841620.1
	R: GCAGCAGGTTCAAAGGCCCG	65			
PgPAP-like	F: TGGATTGGTACGTATTTCACTTCC	42	57	109	–
	R: TCTTCCGGACCATGTGAGTG	55			
PgMYB5-like	F: ATGCGGGAAGAGTTGCAGG	58	57	107	–
	R: GCCTATGGAGCCTGAGAATCA	52			
PgMYB4-like	F: GGATCAACTACCTGCGTCCC	60	58	116	–
	R: TCGACCAGCAATCAAGGACC	55			
PgbHLH	F: CTTCATCGACCACCAACCCC	60	58	101	–
	R: GCGAGTTGAAACGAGGGTGG	60			
PgRPSII	F: TCAATTTGTGAGGGTCGTTCT	43	58	111	Ophir et al., 2014
	R: GATTCAAGAGTAGTAACCGATTCCA	40			

3. Results and discussion

3.1. Phenolic compound profiles during fruit development

Polyphenol composition in plant varies enormously depending predominantly on genotype, development and environmental conditions [60,61]. Many studies investigated the pomegranate phenolic compounds present in leaf, flower and in fruit tissues, but there is still a lack of information on how their composition can change during the development of the fruit. In the present work we performed a LC-PDA-MS analysis to monitor 34 phenolic compounds in leaves, flowers and during fruit development, focussing on gallotannins, galloyl esters, flavonols and anthocyanins, which were identified based on their retention time (rt), absorbance spectrum (PDA) and the observed accurate mass of the molecular ion ([M − H]-) (Table 3).

Log-transformed peak areas for each of these 34 metabolites were used for Principal Component Analysis (PCA), to investigate the relations among the tissues based on their phenolic composition (Fig. 2). Samples of both cultivars clustered with respect to the tissue typology, with leaves and flowers in peripheral position and fruit aril maturation stages showing a relative close relation, especially the turning and ripe stages of fruit development (Fig. 2a). When limiting the PCA to the aril samples only (Fig. 2b), we observed a major differentiation due to fruit ripening stages (PC 1, explaining 74 % of the variation) followed by differences between Valenciana and Wonderful cultivars (PC2, explaining 18 % of the variation).

The comparative analysis of phenolic composition across the sampled tissues showed specific metabolite patterns for both leaf, flower, and fruit tissues (Fig. 3). For both Valenciana and Wonderful, during the fruit development we observed a change in the plant phenolic metabolism from hydrolysable tannins, in which punicalagin and ellagic acid were predominant, to the flavonoid segment, in which the content of anthocyanins raised. Ellagitannins and gallotannins were relative high in both leaves and flowers and decreased in arils during maturation, as previously observed from the analysis of the pomegranate juice during fruit development [62]. Punicalagins (compounds number 1 and 2 in Table 3), the most important ellagitannins in pomegranate, were highest in the flower of both cultivars. Moreover, ellagic acid (3) and ellagic acid hexoside (6), higher in Wonderful than in Valenciana, were markedly higher in seed-containing samples (F + S) compared to the corresponding seed-lacking samples (F) of turning and red fruits. Among the flavonoids, rutin (26) was mainly detected in leaf tissue (Fig. S1), epicatechin (28) increased during fruit development (from Unripe to Ripe stage), while catechin (27) showed an opposite trend. The presence of seed in the aril samples lead to increased catechin contents, indicating that this compounds is relatively high in seed. Among the anthocyanins analysed, pelargonidin-3,5-diglucoside (34) was most concentrated in the flower (Fig. S2), in agreement with a previous study on the Wonderful cultivar [30]. As opposed to the hydrolysable tannins, the anthocyanins increased from Unripe to Ripe fruit, thus correlating well with the fruit pigmentation, as documented previously [3]. The increase of both delphinidin-3,5-glucoside (32) and cyanidin-3,5-diglucoside (33) was largest from turning (F + S) to ripe stage. The Ripe arils were characterized by higher levels of these two anthocyanins in Wonderful compared to Valenciana, while in Valenciana the predominant anthocyanin was pelargonidin-3-glucoside (31), as reported for ripe fruit by Gomez-Caravaca et al. [63]. In contrast to the hydrolysable tannins and catechin, the anthocyanin composition did not differ between F and F + S aril samples of the two cultivars, indicating that the seeds do not contain anthocyanins. Our results are in agreement with whose reported by Ben-Simhon et al. [30,52] and Zhao et al. [20], who showed a similar increase in anthocyanins during fruit development except for pelargonidin-3,5-diglucoside (34), which was found mostly in the flower in the present study.

3.2. Pomegranate flavonoid regulatory genes and their expression profile

Four TFs potentially involved in the regulation of flavonoids were identified in available genomic resources for *P. granatum*. Of these, three were members of the MYB family, and one was a bHLH.

The sequences of isolated TFs involved in the regulation of the flavonoid biosynthetic pathway in pomegranate were used to predict, using a homology-based approach, their relationship with different MYB or bHLH clades related to their putative functions (Fig. S3). The MYB TFs share a R2R3 domain with a [D/E]L × 2[R/K] × 3 L × 6 L × 3R motif through which they interact with bHLH proteins [64]. Within the R2R3 domain, three amino-acid residues (arginine (R), valine (V) and alanine (A) with 100(R): 92(V): 90(A) frequencies respectively) are conserved for dicot anthocyanin biosynthesis promoting MYBs [65]. These conserved key amino acid residues are replaced by glycine (G), glutamic acid (E)/aspartic acid (D) and aspartic acid (D) in other MYBs TFs, among which are regulators of proanthocyanidins (PAs). Moreover, an important differentiation among MYBs was reported based on the C-terminal region motifs, which seem to be specific for different functional sub-groups (SGs) [32,14].

The *PgPAP-like* presented two conserved motifs, the ANDV (red box), within the R2R3 domain, and KPRPR [S/T]F, SG 6 at the C-terminal region (Fig. S3). These two motifs exhibit structural features in common among anthocyanin-regulating MYB TFs, as seen for PAP1 and

Table 3
Identification of phenolic compounds during fruit development stages in Valenciana (VL) and Wonderful (WD).

Compound number	Assignment	Molecular formula	rt (min)	HPLC-PDA λmax (nm)	[M-H]- m/z	Calc. mass	Mass deviation (ppm)
Ellagitannins							
1	Punicalagin α [a]	$C_{48}H_{28}O_{30}$	8.29	258, 382	1083.0601	1083.0593	0.74
2	Punicalagin β [a]	$C_{48}H_{28}O_{30}$	10.64	258, 379	1083.0604	1083.0593	1.02
3	Ellagic acid [a]	$C_{14}H_6O_8$	21.96	253, 368	300.9991	300.9990	0.33
4	Ellagic acid pentoside	$C_{19}H_{14}O_{12}$	21.03	253, 362	433.0419	433.0412	1.62
5	Ellagic acid deoxyhexoside	$C_{20}H_{16}O_{12}$	21.45	253, 362	447.0575	447.0568	1.57
6	Ellagic acid hexoside	$C_{20}H_{16}O_{13}$	16.41	253, 362	463.0526	463.0518	1.73
7	Pedunculagin monomeric I	$C_{34}H_{24}O_{22}$	5.55	n.d.	783.0699	783.0686	1.66
8	Pedunculagin monomer II	$C_{34}H_{24}O_{22}$	6.42	n.d.	783.0698	783.0686	1.53
9	Pedunculagin dimer III [b]	$C_{68}H_{48}O_{44}$	13.26	n.d.	1567.1464	1567.1445	1.21
10	Pedunculagin dimer IV [b]	$C_{68}H_{48}O_{44}$	15.17	n.d.	1567.1464	1567.1445	1.21
11	Galloyl HHDP hexose	$C_{27}H_{22}O_{18}$	14.83	n.d.	633.0743	633.0733	1.58
12	HHDP glucose	$C_{20}H_{18}O_{14}$	3.02	n.d.	481.0629	481.0624	1.04
Gallotannins							
13	Gallic acid [a]	$C_7H_6O_5$	4.48	271	169.0144	169.0142	1.18
14	Galloyl glucose	$C_{13}H_{16}O_{10}$	3.50	n.d.	331.0675	331.0671	1.21
15	Digalloyl hexose I isomer I	$C_{20}H_{20}O_{14}$	9.79	n.d.	483.0786	483.0780	1.24
16	Digalloyl hexose I isomer II	$C_{20}H_{20}O_{14}$	10.87	n.d.	483.0791	483.0780	2.28
17	Digalloyl hexose I isomer III	$C_{20}H_{20}O_{14}$	11.43	n.d.	483.0790	483.0780	2.07
18	Digalloyl hexose I isomer IV	$C_{20}H_{20}O_{14}$	16.06	n.d.	483.0789	483.0780	1.86
19	Trigalloylglucose	$C_{27}H_{24}O_{18}$	12.04	n.d.	635.0900	635.0890	1.57
20	Tetragalloylglucose isomer I	$C_{34}H_{28}O_{22}$	20.41	n.d.	787.1015	787.0999	2.03
21	Tetragalloylglucose isomer II	$C_{34}H_{28}O_{22}$	21.15	n.d.	787.1018	787.0999	2.41
22	Tetragalloylglucose isomer III	$C_{34}H_{28}O_{22}$	21.87	n.d.	787.1016	787.0999	2.16
23	Pentagalloylglucose	$C_{41}H_{32}O_{26}$	24.49	n.d.	939.1130	939.1109	2.24
	Gallagyl esters						
24	Punicalin	$C_{34}H_{22}O_{22}$	4.62	n.d.	781.0543	781.0530	1.66
Flavonoids							
25	Naringin	$C_{27}H_{32}O_{14}$	26.70	283, 334	579.1728	579.1719	1.55
26	Rutin [a]	$C_{27}H_{30}O_{16}$	22.21	255, 355	609.1466	609.1461	0.82
27	Catechin	$C_{15}H_{14}O_6$	11.62	n.d.	289.0722	289.0718	1.53
28	Epicatechin	$C_{15}H_{14}O_6$	15.20	n.d.	289.0722	289.0718	1.64
Anthocyanins							
29	Delphinidin-3-glucoside [a]	$C_{21}H_{21}O_{12}$	8.10	276, 521	463.0888	463.0882	1.19
30	Cyanidin-3-glucoside [a]	$C_{21}H_{21}O_{11}$	10.06	280, 323, 516	447.0934	447.0933	0.35
31	Pelargonidin-3-glucoside [a]	$C_{21}H_{21}O_{10}$	11.67	277, 329, 427, 500	431.0988	431.0984	0.97
32	Delphinidin-3,5-diglucoside [a]	$C_{27}H_{31}O_{17}$	4.90	276, 517	625.1417	625.1410	1.02
33	Cyanidin-3,5-diglucoside [a]	$C_{27}H_{31}O_{16}$	6.55	278, 515	609.1478	609.1461	2.73
34	Pelargonidin-3,5-diglucoside [a]	$C_{27}H_{31}O_{15}$	8.20	276, 498	593.1517	593.1512	0.80

Compounds tentatively identified by comparing with reference compounds in literature.
[a] Compounds identified by comparing retentions time, PDA and MS data with reference standards.
[b] Compound appeared as double charged molecular ion. x, detected; n.d., not detected.

PAP2 in *A. thaliana* that enhance the production of anthocyanins [32,65,36]. While in non-anthocyanin regulator MYB factors, the ANDV motif is substituted by a DNEI motif. Accordingly, our phylogenetic analysis showed clustering of *PgPAP-like* with *A. thaliana* PAP orthologues and MYB113, confirming the closely relation to anthocyanin related sub-clade (Fig. 4). The gene expression profile of *PgPAP-like* varied significantly among samples ($p \leq 0.01$) with the lowest expression at unripe stage and the highest at ripe stage in Wonderful (Fig. 5), which profile was also observed for the anthocyanins content in this cultivar (Fig. S2). In particular, the *PgPAP-like* transcriptional profile was significantly correlated with the content of both delphinidin-3,5-diglucoside, cyanidin-3,5-diglucoside, delphinidin-3-glucoside and cyanidin-3-glucoside (Tab S2), in accordance to what reported previously for fruit peel [30,52]. Moreover, the transcriptional profile of *PgPAP-like* was found to be positively correlated with gene expression of *PgCHS* ($p \leq 0.001$) (Tab S3), which encodes the first committed enzyme in the flavonoid pathway and with *PgF*3'5'*H* responsible for the hydroxylation of dihydrokaempferol to dihydromyricetin. The observed correlation with metabolite contents and gene expression profiles highlights the involvement of *PgPAP-like* in different points of the flavonoid-biosynthesis pathway, especially in the regulation of anthocyanin production.

The *PgMYB4-like* exhibited a conserved EAR (ERF-associated amphiphilic repression) suppression sequence LNL[E/D]L at the C-terminus that characterize the MYB clade (SG 4) which encode transcription repressors [32,66]. Their function was proposed as negatively affecting the early steps of phenylpropanoids pathway and in general for the anthocyanin biosynthesis [34,67]. As a consequence, *PgMYB4-like*clustered with *AtMYB3*, *AtMYB4*, *AtMYB7* and *AtMYB32* forming the "repressor clade" (Fig. 4). The *PgMYB4-like* expression profile was markedly different among samples ($p \leq 0.001$): high at flowering and unripe fruit stages and markedly decreased in ripe fruit (Fig. 5). This profile positively correlates with naringin, catechin, and negatively with rutin, while no correlation with anthocyanins was found, suggesting no involvement with the latter biosynthetic pathway. In *A. thaliana* a similar transcriptional pattern was showed for *AtMYB4* (within the MYB4 clade, Fig. 4), and it was postulated to inhibit the expression of cinnamate-4-hydroxylase (C4H) thereby indirectly controlling the balance of floral volatile benzenoid/phenylpropanoid production [34,68]. Likewise, in *Malus domestica* the over-expression of *MdMYB16* inhibited the expression of the anthocyanin biosynthetic pathway structural genes ANS and UFGT, thus affecting anthocyanin production [67]. However, the expression pattern observed for *PgMYB4-like* in the present study was positively correlated only with *PgbHLH* ($p \leq 0.01$) and not with any of the selected structural genes. All these findings may support a different function of *PgMYB4-like* as compared to other MYB genes included in the "repressor clade", being linked to the production of flavonoids other than the anthocyanins.

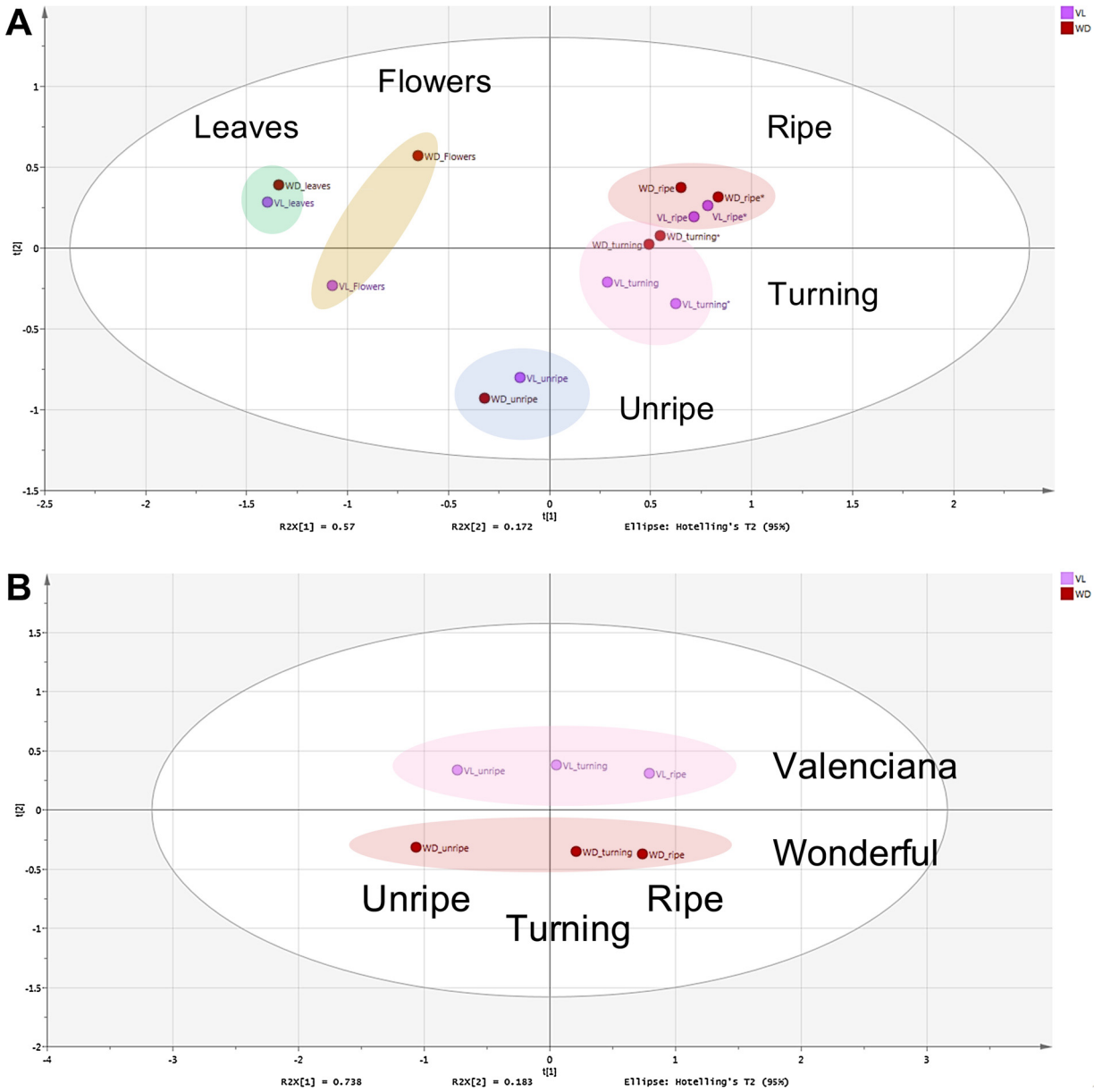

Fig. 2. Principal component analysis (PCA) of Valenciana (VL) and Wonderful (WD) cultivars across different plant tissues (A) and during aril development (B), based on the log-transformed and Pareto-scaled peak areas of 34 phenolic compounds reported in Table 3. The stars indicate stage Ripe F + S.

In the *PgMYB5-like* protein sequence, we identified a C-terminus motif "VNEFFDFTT" and "SYGLEW" (Fig. 4), labelled as SG 26, firstly described in the present study. *PgMYB5-like* shares these motives with *PpMYB7* of *Prunus persica*, *Vitis vinifera* WER-like TFs and *Malus domestica* MYB5-like (Fig. S3). *PpMYB7* belongs to the R2R3-MYB group, not reported for *A. thaliana*. In *P. persica* it regulates the synthesis of proanthocyanidins (PA) eliciting catechins production [69]. PA-related MYBs require a bHLH partner for the trans-activation of PA pathway genes [70,71]. In *P. persica, PpMYB7* was reported to use either *PpbHLH3* and *PpbHLH33* to activate catechin production [69], while in apple fruit *MdMYB9* requires *MdbHLH3* as a partner to regulate the biosynthesis of PAs [72,73]. In the present work, the expression of *PgMYB5-like* showed a tissue-based pattern (Fig. 5), especially for Wonderful, with the highest values in flowers and decreasing during fruit development, when anthocyanins increase. The *PgMYB5-like* transcriptional profile was negatively correlated with epicatechin and strongly with pelargonidin-3,5-diglucoside content ($p \leq 0.001$) which was highest at flowering but no correlation was found with the other anthocyanins. This expression pattern is in accordance with the high transcript level of *Pgr021507.1* (included in the MYB5/WER like cluster, Fig. 4) observed in flower tissue of *P. granatum* cultivar 'Dabenzi' [22]. A close phylogenetic MYB member, the *PpMYB7*, belonging to the MYB5/WER like group described for peach (*P. persica*) fruit, was shown to specifically activate the expression of *PpLAR1* thereby inducing catechin production, but not that of *PpANR* which is known to induce epicatechin production [69]. In the present study, the identified *PgMYB5-like* is mostly expressed at flowering stage and it is not associated with most of flavonoids nor with anthocyanins except for pelargonidin-3,5-diglucoside. However the *PgMYB5-like* transcriptional profile significantly correlated with *PgDFR*, encoding an enzyme which reduces dihydroflavonols to corresponding colourless leucoanthocyanidins. Moreover, we observed a positive correlation between *PgMYB5-like* and *PgbHLH* expression suggesting the presence of an interaction between these two TFs as for other MYB members. All these findings provide new probable functions for *PgMYB5-like* transcription factor beyond the regulation of anthocyanin biosynthesis pathway, which

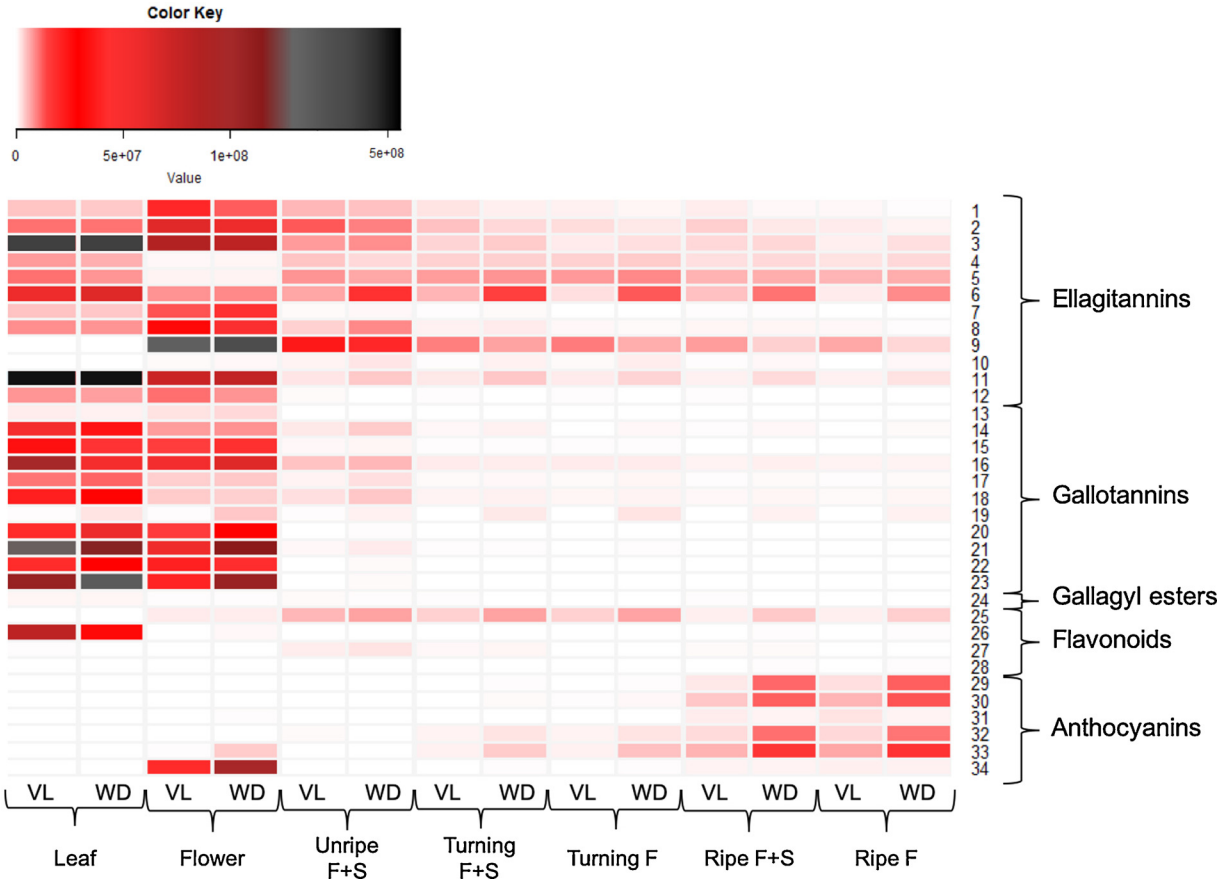

Fig. 3. Peak areas heat map of phenolic compounds found in Valenciana (VL) and Wonderful (WD) in sampled tissues: leaf, flower, unripe whole arils (F + S), turning whole arils (F + S), turning arils flesh (F), ripe whole arils (F + S) and ripe arils flesh (F). Numbers on the left refer to the compounds reported in Table 3.

contributes to our understanding of the MYB-SG26 group, which was only partially investigated.

The bHLH proteins are characterized by a DNA binding basic-Helix-Loop-Helix domain and, in plants, they can act as homo- or heterodimers, associate with proteins from other protein families, or form MYB/bHLH complexes to regulate many cellular key processes [32,74]. Among bHLHs, the members of plant sub-group IIIf are involved in flavonoid/anthocyanin biosynthesis (in *Arabidopsis AtMYC1* and *AtTT8*) and trichome initiation (*AtGL3*) [75]. In the present work, the identified *PgbHLH* exhibited a close relation with *PpbHLH* 3 which is homologous of *A. thaliana* TT8 gene, a key regulator of anthocyanin and proanthocyanidin biosynthesis [76] (Figs. S4 and S5). The transcriptional levels of *PgbHLH* differed significantly ($p \leq 0.001$) across samples (Fig. 5). In Wonderful its level was more or less constantly high except for leaves, while in Valenciana the expression level was highest at flowering and decreased during fruit ripening, as previously reported for the Dabenzi cultivar [22]. This expression pattern was positively correlated with naringin and negatively with rutin content, while no correlation was found with anthocyanins content. The latter finding is in agreement with a previous investigation on Wonderful cultivars with respect to cyanidin derivates [30], while the bHLH-flavonoids association has not been investigated in pomegranate so far. Moreover, the *PgbHLH* transcriptional profile was correlated with *PgMYB5-like* and *PgMYB4-like* expression, suggesting an interaction of bHLH with these MYB members with an uncertain function and not with *PgPAP-like* which is known to regulate anthocyanins biosynthetic pathway. Moreover *PgbHLH* expression was correlated with all the four structural genes analysed in the present study *PgDFR, PgCHS, PgF*3'5'*H* and *PgUFGT*. This result strongly suggests a key role of this TF along the flavonoid-biosynthesis pathway.

3.3. Flavonoid structural genes expression in pomegranate tissues

In addition to the expression of TFs, the expression of structural genes involved in the biosynthetic pathway of flavonoids was assessed measuring the transcripts abundances by RT-qPCR (Fig. 6). Differently from TFs, for the most of the selected flavonoid structural genes their expression profile was highly correlated with anthocyanins. *PgCHS* expression varied significantly ($p \leq 0.001$) across tissues and cultivars. This gene was highly up-regulated in ripe arils of Wonderful, while its expression could not be detected for ripe arils of Valenciana. Previously, the expression level of *PgCHS* was shown to be not significantly correlated with the fruit peel colour (assessed as total cyanidin derivates) and the timing of colour appearance in both Wonderful and P.G.135-36 accessions [30]. Zhao et al. [20] documented the presence of two peaks of *PgCHS* transcript abundance, i.e. at early development and at fruit ripening, and argued that its expression was not directly associated with the increase in anthocyanins upon fruit maturation. However, in the present study, we found a slightly higher expression levels in flower of both accessions, while, among the identified anthocyanins, only pelargonidin-3,5-diglucoside (34) was relatively high. However, at ripening stage (F + S and S), which showed the highest anthocyanins (29-34) and epicatechin levels (28), *PgCHS* expression was significantly up-regulated in Wonderful with respect to Valenciana. The transcriptional profile of *PgCHS* was highly significantly correlated ($p \leq 0.001$) with most of anthocyanins content: delphinidin-3,5-diglucoside, cyanidin-3,5-diglucoside, delphinidin-3-glucoside, pelargonidin-3,5-diglucoside and cyanidin-3-glucoside. While it showed lower correlation with epicatechin. Moreover, *PgCHS* expression was strongly correlated with all the selected structural genes ($p \leq 0.001$) and, among TFs, with *PgbHLH* and *PgPAP-like*. All these findings may reflect

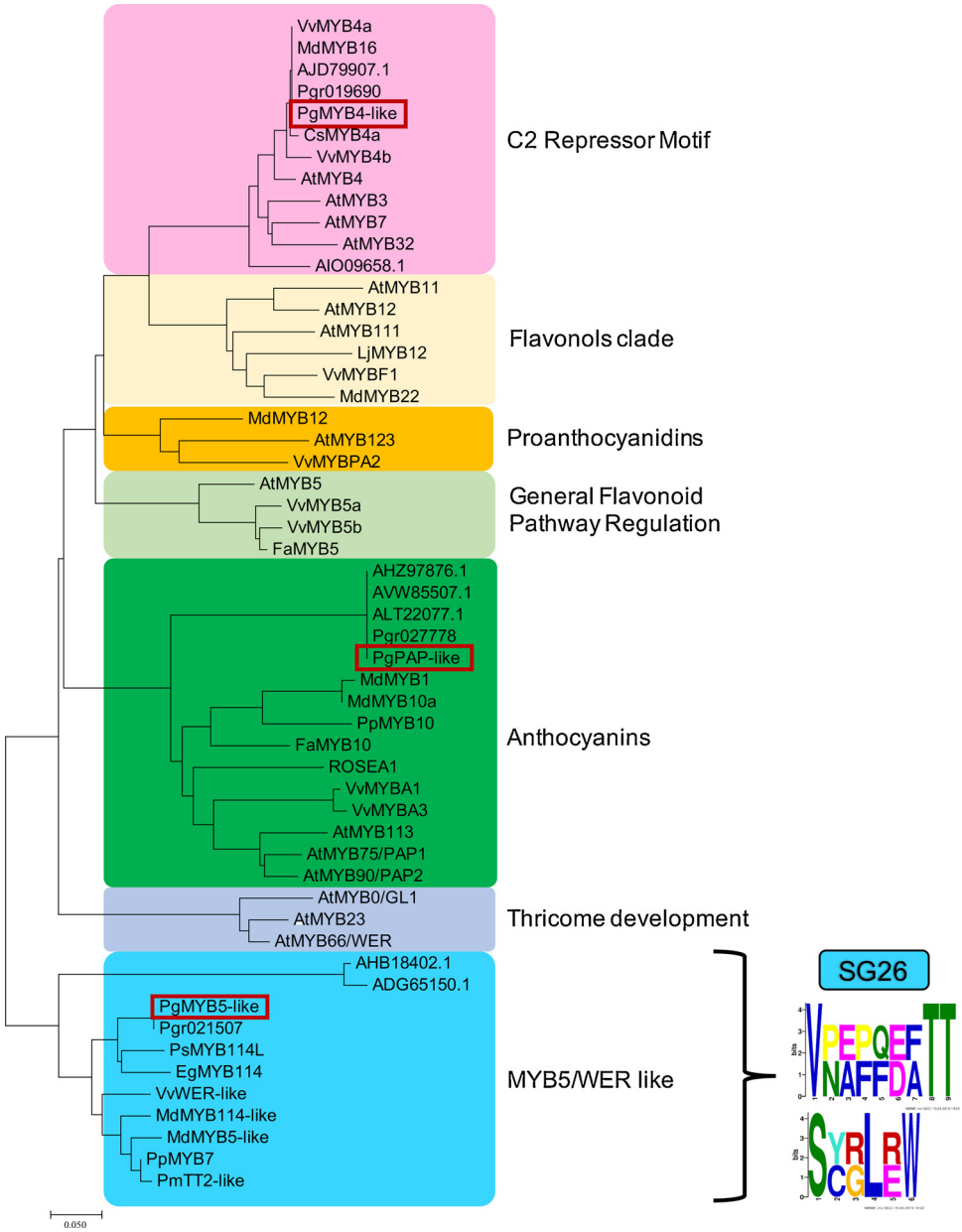

Fig. 4. Neighbour-Joining tree analysis of *PgMYBs* (red boxes) identified in this study respect to MYB-domain proteins in other species. Motif discovery analysis with MEME suite of the *PgMYB5-like* C-terminal region that lead to the designation of the labelled "Sub-group 26".

its direct involvement in several pomegranate flavonoid biosynthesis pathway steps especially within the anthocyanins class.

With regard to *PgF*3'5'*H,* its transcriptional levels varied significantly ($p \leq 0.01$) across samples, especially at ripe stage, with an almost 5 times higher level for Wonderful compared to Valenciana. This expression profile was correlated ($p \leq 0.05$) with the higher delphinidins content detected and also with cyanidin-3,5-diglucoside. Moreover, *PgF*3'5'*H* transcriptional profile was strongly correlated ($p \leq 0.001$) with *PgCHS* and *PgDFR*, while, among TFs, with *PgPAP-like* and *PgbHLH* ($p \leq 0.05$). F3'5'H determines the hydroxylation pattern of the B-ring of dihydroflavonols and it is responsible for the production of myricetin-type of flavonols and delphinidin-based anthocyanins [77]. The association pattern observed in the present study provide a further evidence of its role as a key enzyme in anthocyanidin core structure determination and thus in the colour of flowers and fruits [24].

The expression of *PgDFR* varied with high significance ($p \leq 0.001$) with respect to both cultivar and tissues, with its highest value measured at ripe stage of Wonderful. Similarly, a Wonderful landrace accession was previously reported to exhibit the highest *PgDFR* levels in the fruit peel at ripe stage [30]. In addition, DFR showed a higher level of expression in black peel pomegranates compared to red, green and white cultivars, corresponding to the anthocyanin content distribution among these cultivars [21]. In the hard-seeded pomegranate cultivar 'Dabenzi' the up-regulation of DFR gene (Pgr021399 - OWM75048.1 protein) corresponded to the accumulation of anthocyanins in the outer seed coat [22]. Similarly, in the present study, the DFR transcriptional profile was correlated with all anthocyanins content, except for pelargonidin-3-glucoside and we observed the highest expression of *PgDFR* in ripe arils of Wonderful. The Pearson correlation was significantly higher ($p \leq 0.01$) for cyanidin-3,5-diglucoside, delphinidin-3-glucoside and pelargonidin-3,5-diglucoside, while it was lower ($p \leq 0.01$) for delphinidin-3,5-glucoside and cyanidin-3-diglucoside. Its transcriptional profile was also correlated significantly with the transcript levels of *PgCHS*, and *PgF*3'5'*H* ($p \leq 0.001$), with *PgUFGT* and *PgbHLH* ($p \leq 0.01$) and less with *PgMYB5-like* ($p \leq 0.05$) claiming a key role in the anthocyanins biosynthesis pathway.

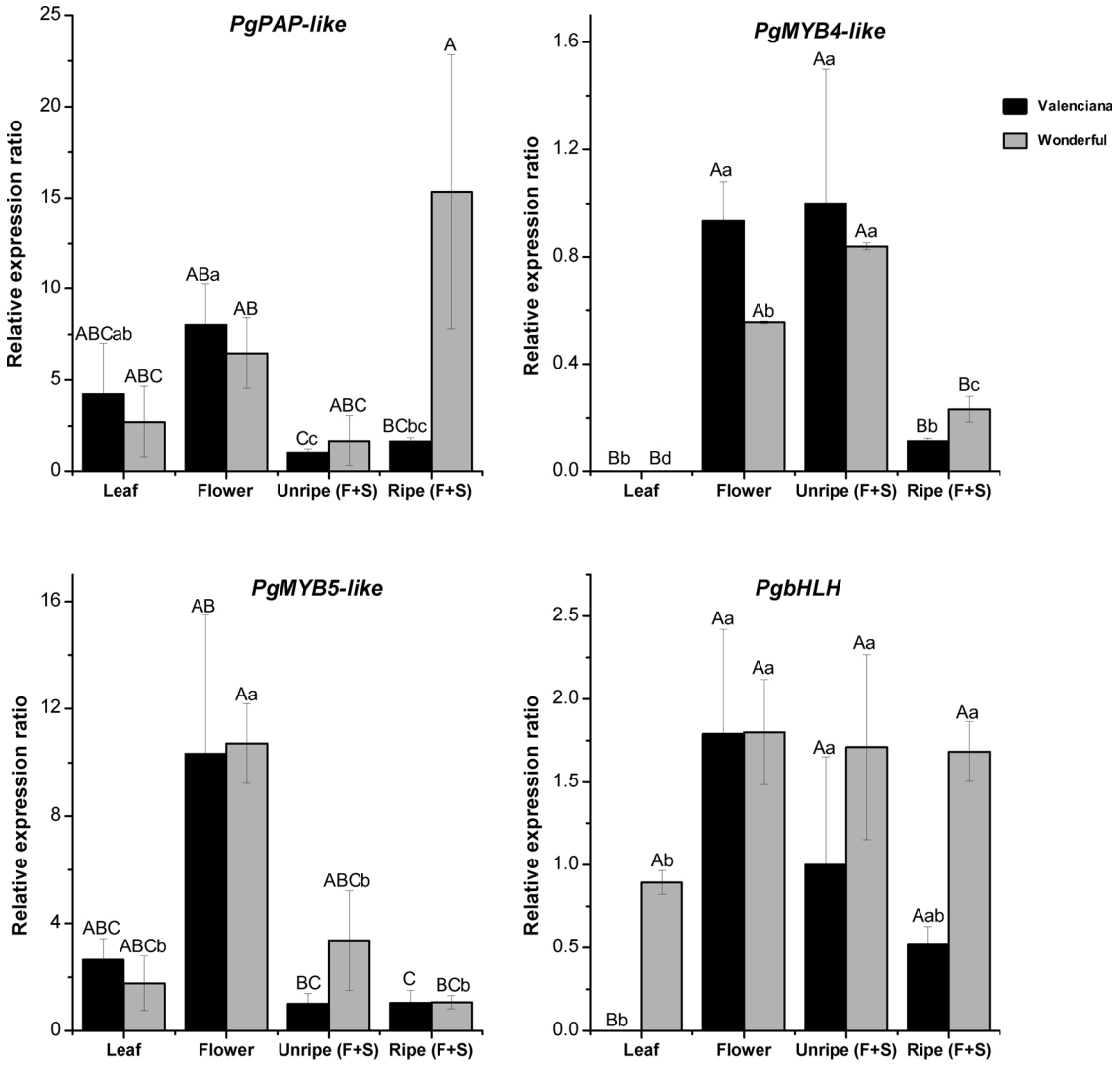

Fig. 5. Relative expression of flavonoid-associated TFs in different tissues in Valenciana and Wonderful cultivars. The relative expression ratio is calculated as the fold increase relative to unripe arils (F + S) of Valenciana. The error bars represent the standard error of the mean of three biological replicates. Upper or lower case letters indicate only significant differences according to ANOVA (p value $\leq$ 0.05) among all samples or among tissues of each genotype, respectively.

UDP-glucoside flavonoid glucosyltransferase (UFGT) is an important enzyme in flavonoid biosynthesis because it stabilizes anthocyanins by attaching sugar moieties to the flavonoid aglycon [78]. In our study the expression levels of *PgUFGT* varied slightly significantly across tissues and cultivars ($p \leq$ 0.05) with highest expression values in ripe stage arils of Wonderful, in which *PgUFGT* average expression was almost twice of that in Valenciana. In peach flower the anthocyanin content and the expression levels of both *DFR* and *UFGT* genes were shown to increase during fruit development [79]. In the pomegranate Dabenzi cultivar the gene expression of *PgUFGT* (*Pgr022819* - OWM79407.1 protein), like that of DFR, was shown to coincide with the accumulation of anthocyanins in the outer seed coat during development [22]. The expression pattern of *PgUFGT* observed in the present study was similar to that observed for the Dabenzi cultivar, with major expression in flowers and ripe arils for Wonderful. Its expression profile was significantly correlated ($p \leq$ 0.05) with cyanidin-3,5-diglucoside and delphinidin-3-glucoside, while it was negatively correlated ($p \leq$ 0.05) with rutin content. The correlation ($p \leq$ 0.01) with *PgbHLH* and *PgDFR* ($p \leq$ 0.05) and not with *PgPAP-like* evidences its involvement only in the final step of anthocyanins pathway.

3.4. Functional studies in N. benthamiana

In order to disentangle the function of the newly identified *PgMYB5-like* TF and its interaction with *PgbHLH* the two transcripts were transiently expressed in the model plant *N. benthamiana* using ROS1 + DEL construct as reference system for the induction of anthocyanins [45]. When *N. benthamiana* leaves were agroinfiltrated with either *PgMYB5-like* or *PgbHLH* alone, no leaf colour modification was observed (Fig. S6). In contrast, a marked increase in colour was observed with the combined Myb + bHLH gene constructs *PgMYB5-like* + *PgbHLH* or ROS1 + DEL (Fig. 7). The presence of the both pomegranate TFs produced a brown leaf colour (Fig. 7C and D), while the presence of both snapdragon TFs resulted in a purple colouring (Fig. 7E and F). For both TF combinations the colour intensity increased with time after infiltration. By microscopical analysis of the brown areas of *PgMYB5-like* + *PgbHLH* co-infiltrated leaves we detected an extensive abundance of possibly vacuolar metabolite inclusions within the epidermal cells (Fig. 7G and H).

N. benthamiana leaves infiltrated with pomegranate genes were sampled at different times (4 or 6 days) after infiltration and their metabolite compositions compared using an essentially untargeted LC-PDA-MS approach, in order to functionally analyse the *P. granatum* TFs on the leaf metabolome with focus on (poly)phenols. The PCA of

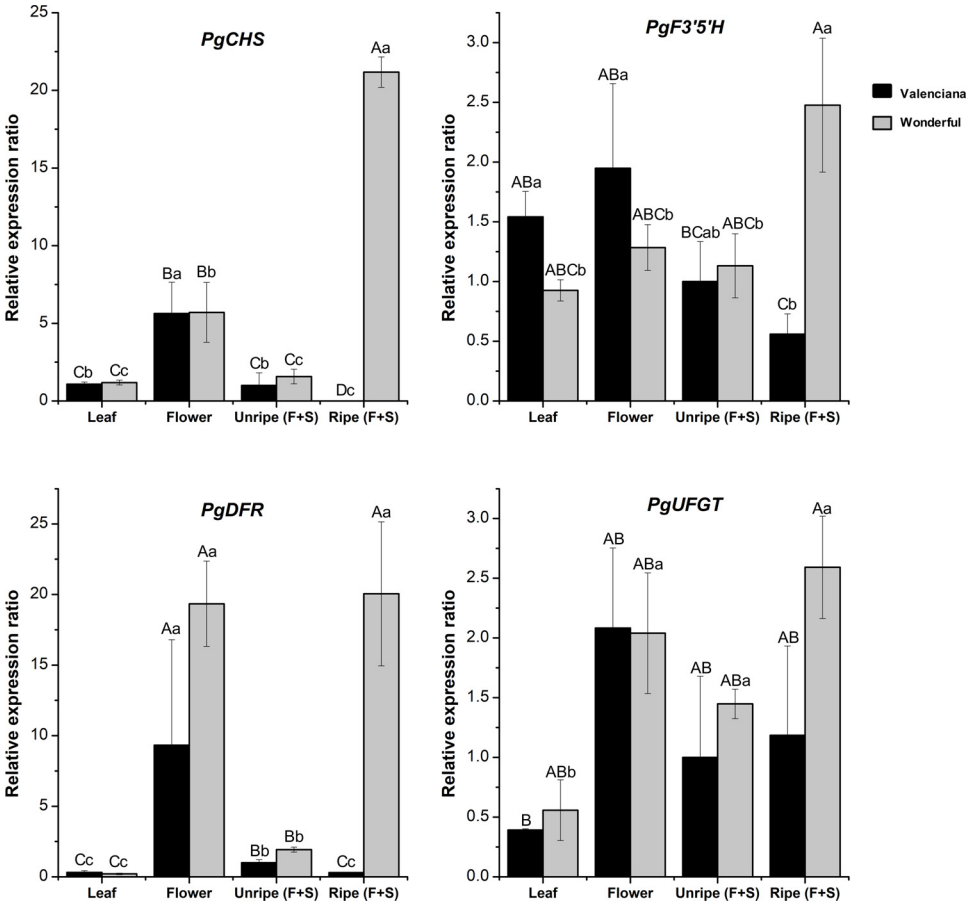

Fig. 6. Expression of structural flavonoid genes in different tissues in Valenciana and Wonderful cultivars. *PgCHS:* Chalcone synthase; *PgF3'5'H:* Flavonoid 3',5'-hydroxylase; *PgDFR:* dihydroflavonol 4-reductase; *PgUFGT:* UDP-glucoside: flavonoid glucosyltransferase. The relative expression ratio is expressed as the fold increase relative to unripe (F + S) of Valenciana. The error bars represent the standard error of the mean of three biological replicates. Upper or lower case letters indicate only significant differences according to ANOVA (p value ≤ 0.05) among all samples or among tissues of each genotype, respectively.

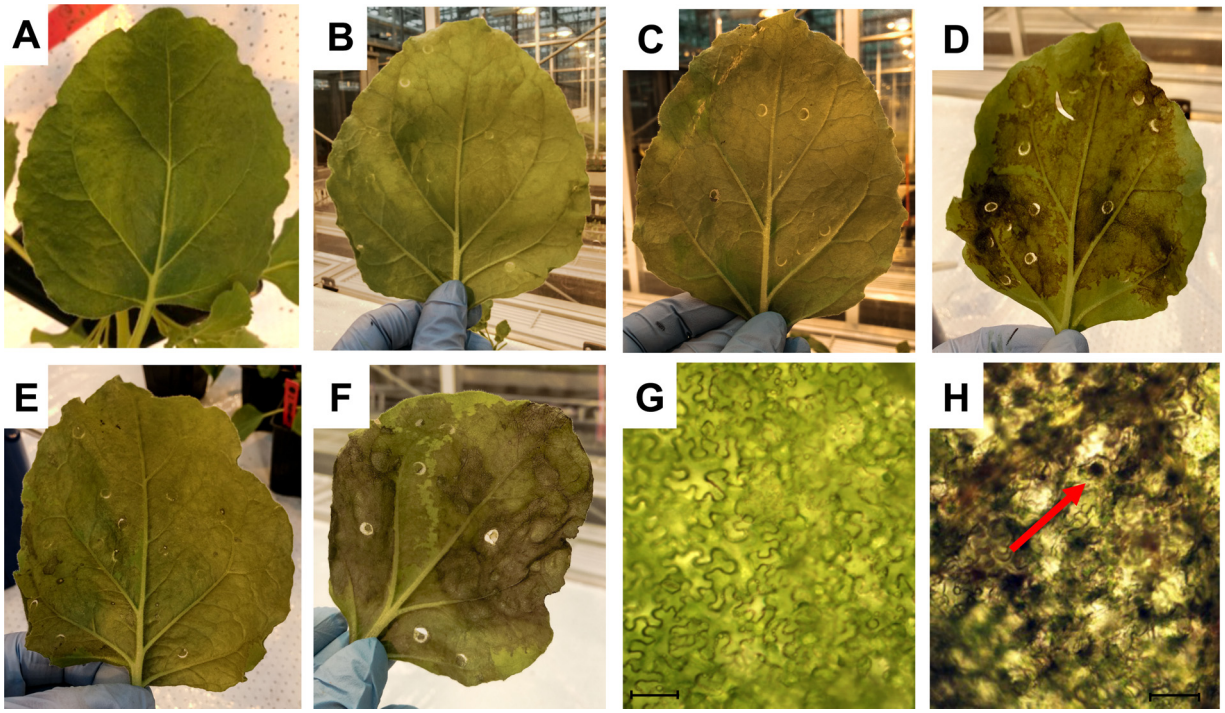

Fig. 7. *N. benthamiana* leaves wild type (A), agroinfiltrated with pBIN empty vector as negative control (B), or with *PgMYB5-like* + *PgbHLH* after 4 (C) or 6 (D) days and with ROS1 + DEL after 4 (E) or 6 (F). Microscopical analysis of epidermal cells of agroinfiltrated leaves with pBIN empty vector (G) or with *PgMYB5-like* + *PgbHLH* (H) after 6 days, arrow indicates possible vacuolar inclusions of metabolites.

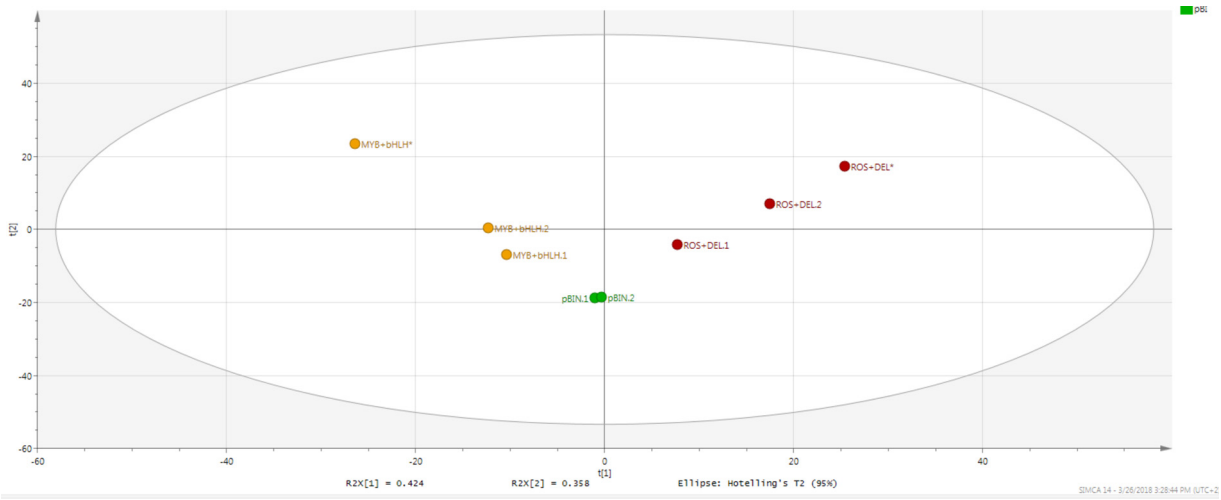

Fig. 8. Principal component analysis based on 664 metabolites of whole *N. benthamiana* leaves transiently co-transformed with *PgMYB5-like* + *PgbHLH* (yellow colour) or ROS1 + DEL (red colour) or pBIN empty vector (green colour) constructs harvested after 4 (pBIN-1, MYB-bHLH-1 and ROS-DEL-1) or 6 days (pBIN-2, MYB-bHLH-2 and ROS-DEL-2) after agroinfiltration. Stars represent samples specifically taken from the pigmented areas of leaves after 6 days of TF-agroinfiltration.

infiltrated leaves based on 664 metabolites (Table S4) showed a clear time-dependent and opposite deviation of *N. benthamiana* leaves infiltrated with each combined TF construct, indicating differential effects on metabolism as compared to the leaves with pBIN empty-vector used as negative control. The biggest effects of infiltrated TFs were observed in the pigmented leaf areas (Fig. 8).

PgMYB5-like + *PgbHLH* agroinfiltrated *N. benthamiana* leaves accumulated several compounds that are derived from the flavonoid pathway (Fig. 9B). Among these compounds a series of conjugated dihydroflavonols, including glycosylated and methylated dihydromyricetin, dihydrokaempferol, dihydroquercetin could be identified (Table S4). All the identified dihydroflavonol compounds accumulated with a higher extent in the presence of *PgMYB5-like* + *PgbHLH* compared to ROS1 + DEL snapdragon genes for which lower levels were detected, except for dihydroquercetin di-methyl ether hexoside which was not detected in ROS1 + DEL agroinfiltrated plants. These lower levels, in the presence of ROS1 + DEL, are likely due to the fact that in these plants the produced dihydroflavonols can be partly converted into anthocyanins. The LC-PDA profiles at 510 nm confirmed this finding showing a single peak, corresponding to delphinidin-3-rutinoside, in ROS1 + DEL agroinfiltrated plants (Fig. 9A) and this is in agreement to a previous study using the same snap dragon TFs [45]. In contrast, no anthocyanins were detected in leaves either transiently expressing the pomegranate *PgMYB5-like* + *PgbHLH* TF-genes or agroinfiltrated with the empty pBIN vector (Fig. 9A) neither in the single gene constructs (Table S4).

However, agroinfiltrated leaves with ROS1 + DEL resulted in the accumulation of quercetin-3-O-rutinoside (rutin) and less for kaempferol-3-O-rutinoside but they not accumulated or less with pomegranate TFs. All these findings suggest that in *N. benthamiana PgMYB5-like* + *PgbHLH* activate the pathway up to F3H and subsequently F3'H and F3'5'H, while both DFR/ANS and FLS are not activated.

The brown colour of the *PgMYB5-like* + *PgbHLH* infiltrated leaves is likely due to oxidation and polymerization of unstable, non-conjugated intermediates of the pathway towards anthocyanidins.

4. Conclusions

In the present study, the metabolic profiling of two major pomegranate cultivars, Wonderful and Valenciana, revealed an ample presence of hydrolysable tannins compounds (ellagitannins and gallotannins) in leaves and flowers which decreased during fruit maturation. Contrary to these hydrolysable tannins, the anthocyanins increased during fruit development, with a higher content in Wonderful resulting in its more intense purple colour compared to Valenciana. In view of the well-documented role of MYB TFs in the regulation of flavonoid biosynthesis in fruits, including pomegranate, we here identified a series of flavonoid-pathway TFs in pomegranate. Based on its sequence homology with known repressor TFs, we speculate about a possible role of *PgMYB4* as repressor of flavonoid biosynthesis, but its expression profile could only highlight the lack of correlation with anthocyanins and could not confirm a precise repressor role in the flavonoid biosynthesis. As regards to *PgPAP-like* MYB gene we suggest a possible function as a stimulator of anthocyanin biosynthesis in pomegranate, based on its corresponding expression pattern with the *PgCHS* and *PgF*3'5'*H* structural genes and the content of the most of anthocyanins. In addition, we functionally characterized a member of MYB5 TFs (absent in *A. thaliana*), which is involved in the flavonoid pathway but with a different function with respect to the characterized MYB groups. Gene expression and metabolomics analyses of agroinfiltrated *N. benthamiana* leaves revealed that *PgMYB5-like* strongly interacts with *PgbHLH* probably activating F3H, F3'H and F3'5'H resulting in the production of various conjugates of dihydroflavonols, i.e. anthocyanin-pathway intermediates, as well as unstable compounds causing brown leaf colouring. This effect of *PgMYB5-like* + *PgbHLH* was markedly different with respect to ROS1 + DEL agroinfiltration, which induced a marked anthocyanin production in these *N. benthamiana* leaves. We suggest that these newly characterized flavonoid pathway transcription factors play a key role in the regulation of catechins and/or flavonols contents in pomegranate. Unlike previous studies on pomegranate TFs, this work provides an extensive biochemical/metabolomics characterization of the fruit development stages. A combination of metabolomics, transcriptomics and genetic approaches will enable further enhancing our knowledge of flavonoid biosynthesis mechanisms in pomegranate and this knowledge may be used for supporting breeding efforts towards developing new pomegranate cultivars with tailored polyphenol composition.

Funding

This work was financed with funding provided by Catania section of the Istituto per i Sistemi Agricoli, e Forestali del Mediterraneo (CNR-ISAFOM).

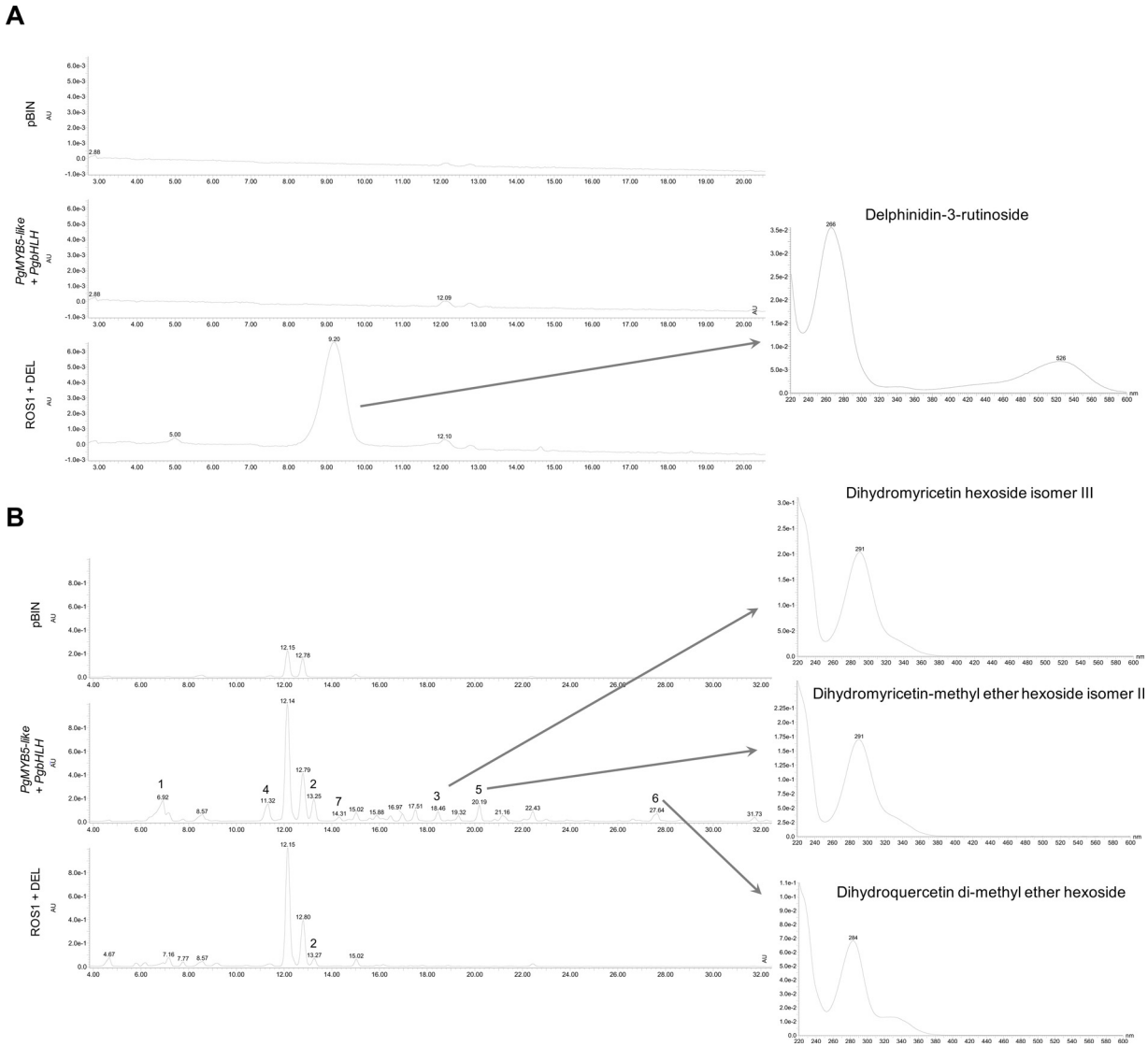

Fig. 9. Metabolite profiles of *N. benthamiana* leaves extracts infiltrated with pBIN (negative control), *PgMYB5-like* + *PgbHLH* and ROS1 + DEL detected by HPLC-PDA at 520 nm (A) and 280 nm (B). Inserted panel shows the UV–vis absorbance spectrum of the delphinidin-3-rutinoside peak. Values above peaks correspond to their observed retention time (min) and lambda-max; number of indicated peaks refer to the compounds reported in Table S4. The two small 520-nm peaks visible in A at retention times 12.1 min and 12.8 min are due to a-specific absorbance by the two corresponding phenylpropanoid peaks in B.

Declaration of Competing Interest

The authors declare that they have no conflict of interest.

Acknowledgements

The authors kindly thank Pietro Calderaro for field managing and the lab assistants of Bioscience-WUR for their valuable contribution to this research: Bert Schipper for running the LC-PDA-MS system, Henriette van Eekelen for helping in the LCMS data processing and Adele van Houwelingen for her help in the DNA and RNA extractions.

Appendix A. Supplementary data

Supplementary material related to this article can be found, in the online version, at doi:https://doi.org/10.1016/j.plantsci.2020.110563.

References

[1] P. Mena, C. García-Viguera, J. Navarro-Rico, D.A. Moreno, J. Bartual, D. Saura, et al., Phytochemical characterisation for industrial use of pomegranate (Punica granatum L.) cultivars grown in Spain, J. Sci. Food Agric. 91 (2011) 1893–1906, https://doi.org/10.1002/jsfa.4411.

[2] U.A. Fischer, R. Carle, D.R. Kammerer, Identification and quantification of phenolic compounds from pomegranate (Punica granatum L.) peel, mesocarp, aril and differently produced juices by HPLC-DAD-ESI/MS n, Food Chem. 127 (2011) 807–821, https://doi.org/10.1016/j.foodchem.2010.12.156.

[3] M.I. Gil, F.A. Tomas-Barberan, B. Hess-Pierce, D.M. Holcroft, A.A. Kader, Antioxidant activity of pomegranate juice and its relationship with phenolic composition and processing, J. Agric. Food Chem. 48 (2000) 4581–4589, https://doi.org/10.1021/jf000404a.

[4] D. Tibullo, N. Caporarello, C. Giallongo, C.D. Anfuso, C. Genovese, C. Arlotta, et al., Antiproliferative and antiangiogenic effects of Punica granatum juice (PGJ) in multiple myeloma (MM), Nutrients 8 (2016) 611, https://doi.org/10.3390/nu8100611.

[5] N.P. Seeram, W.J. Aronson, Y. Zhang, S.M. Henning, A. Moro, R.P. Lee, et al., Pomegranate ellagitannin-derived metabolites inhibit prostate cancer growth and localize to the mouse prostate gland, J. Agric. Food Chem. 55 (2007) 7732–7737, https://doi.org/10.1021/jf071303g.

[6] A.M. Gómez-Caravaca, V. Verardo, M. Toselli, A. Segura-Carretero, A. Fernández-Gutiérrez, M.F. Caboni, Determination of the major phenolic compounds in pomegranate juices by HPLC-DAD-ESI-MS, J. Agric. Food Chem. 61 (2013) 5328–5337, https://doi.org/10.1021/jf400684n.

[7] V. Brighenti, S.F. Groothuis, F.P. Prencipe, R. Amir, S. Benvenuti, F. Pellati, Metabolite fingerprinting of Punica granatum L. (pomegranate) polyphenols by means of high-performance liquid chromatography with diode array and

electrospray ionization-mass spectrometry detection, J. Chromatogr. A 1480 (2017) 20–31, https://doi.org/10.1016/j.chroma.2016.12.017.
[8] R. Koes, W. Verweij, F. Quattrocchio, Flavonoids: a colorful model for the regulation and evolution of biochemical pathways, Trends Plant Sci. 10 (2005) 236–242, https://doi.org/10.1016/j.tplants.2005.03.002.
[9] B.A. Bohm, Introduction to flavonoids, Introd. to Flavonoids, (1998) https://www.cabdirect.org/cabdirect/abstract/19990310974.
[10] M. Mochizuki, S.I. Yamazaki, K. Kano, T. Ikeda, Kinetic analysis and mechanistic aspects of autoxidation of catechins, Biochim. Biophys. Acta – Gen. Subj. 1569 (2002) 35–44, https://doi.org/10.1016/S0304-4165(01)00230-6.
[11] L. Pourcel, J.-M. Routaboul, V. Cheynier, L. Lepiniec, I. Debeaujon, Flavonoid oxidation in plants: from biochemical properties to physiological functions, Trends Plant Sci. 12 (2007) 29–36, https://doi.org/10.1016/J.TPLANTS.2006.11.006.
[12] A. Rauf, M. Imran, T. Abu-Izneid, Iahtisham-Ul-Haq, S. Patel, X. Pan, et al., Proanthocyanidins: a comprehensive review, Biomed. Pharmacother. 116 (2019) 108999, , https://doi.org/10.1016/j.biopha.2019.108999.
[13] B. Winkel-Shirley, Flavonoid biosynthesis. A colorful model for genetics, biochemistry, cell biology, and biotechnology, Plant Physiol. 126 (2001) 485–493, https://doi.org/10.1104/pp.126.2.485.
[14] F. Quattrocchio, A. Baudry, L. Lepiniec, E. Grotewold, The regulation of flavonoid biosynthesis, Sci. Flavonoids, Springer New York, New York, NY, 2006, pp. 97–122, https://doi.org/10.1007/978-0-387-28822-2_4.
[15] R.A. Dixon, G.M. Pasinetti, Flavonoids and isoflavonoids: from plant biology to agriculture and neuroscience, Plant Physiol. 154 (2010) 453–457, https://doi.org/10.1104/pp.110.161430.
[16] V. Lobo, A. Patil, A. Phatak, N. Chandra, Free radicals, antioxidants and functional foods: impact on human health, Pharmacogn. Rev. 4 (2010) 118–126, https://doi.org/10.4103/0973-7847.70902.
[17] W. Zhu, Q. Jia, Y. Wang, Y. Zhang, M. Xia, The anthocyanin cyanidin-3-O-β-glucoside, a flavonoid, increases hepatic glutathione synthesis and protects hepatocytes against reactive oxygen species during hyperglycemia: involvement of a cAMP-PKA-dependent signaling pathway, Free Radic. Biol. Med. 52 (2012) 314–327, https://doi.org/10.1016/j.freeradbiomed.2011.10.483.
[18] S. Kumar, A.K. Pandey, Chemistry and biological activities of flavonoids: an overview, Transfus. Apher. Sci. 2013 (2013) 1–16, https://doi.org/10.1155/2013/162750.
[19] R. Ophir, A. Sherman, M. Rubinstein, R. Eshed, M.S. Schwager, R. Harel-Beja, et al., Single-nucleotide polymorphism markers from de-novo assembly of the pomegranate transcriptome reveal germplasm genetic diversity, PLoS One 9 (2014) e88998, , https://doi.org/10.1371/journal.pone.0088998.
[20] X. Zhao, Z. Yuan, L. Feng, Y. Fang, Cloning and expression of anthocyanin biosynthetic genes in red and white pomegranate, J. Plant Res. 128 (2015) 687–696, https://doi.org/10.1007/s10265-015-0717-8.
[21] S. Rouholamin, B. Zahedi, F. Nazarian-Firouzabadi, A. Saei, Expression analysis of anthocyanin biosynthesis key regulatory genes involved in pomegranate (Punica granatum L.), Sci. Hortic. (Amsterdam) 186 (2015) 84–88, https://doi.org/10.1016/j.scienta.2015.02.017.
[22] G. Qin, C. Xu, R. Ming, H. Tang, R. Guyot, E.M. Kramer, et al., The pomegranate (Punica granatum L.) genome and the genomics of punicalagin biosynthesis, Plant J. 91 (2017) 1108–1128, https://doi.org/10.1111/tpj.13625.
[23] Z. Yuan, Y. Fang, T. Zhang, Z. Fei, F. Han, C. Liu, et al., The pomegranate (Punica granatum L.) genome provides insights into fruit quality and ovule developmental biology, Plant Biotechnol. J. 16 (2018) 1363–1374, https://doi.org/10.1111/pbi.12875.
[24] Y. Tanaka, Flower colour and cytochromes P450, Phytochem. Rev. 5 (2006) 283–291, https://doi.org/10.1007/s11101-006-9003-7.
[25] J.I. Nakajima, Y. Tanaka, M. Yamazaki, K. Saito, Reaction mechanism from leucoanthocyanidin to anthocyanidin 3-glucoside, a key reaction for coloring in anthocyanin biosynthesis, J. Biol. Chem. 276 (2001) 25797–25803, https://doi.org/10.1074/jbc.M100744200.
[26] N. Kovinich, A. Saleem, J.T. Arnason, B. Miki, Functional characterization of a UDP-glucose:flavonoid 3-O- glucosyltransferase from the seed coat of black soybean (Glycine max (L.) Merr.), Phytochemistry 71 (2010) 1253–1263, https://doi.org/10.1016/j.phytochem.2010.05.009.
[27] L. Jaakola, New insights into the regulation of anthocyanin biosynthesis in fruits, Trends Plant Sci. 18 (2013) 477–483, https://doi.org/10.1016/j.tplants.2013.06.003.
[28] W. Xu, C. Dubos, L. Lepiniec, Transcriptional control of flavonoid biosynthesis by MYB-bHLH-WDR complexes, Trends Plant Sci. 20 (2015) 176–185, https://doi.org/10.1016/j.tplants.2014.12.001.
[29] M. Montefiori, C. Brendolise, A.P. Dare, L.W. Kui, K.M. Davies, R.P. Hellens, et al., In the Solanaceae, a hierarchy of bHLHs confer distinct target specificity to the anthocyanin regulatory complex, J. Exp. Bot. 66 (2015) 1427–1436, https://doi.org/10.1093/jxb/eru494.
[30] Z. Ben-Simhon, S. Judeinstein, T. Nadler-Hassar, T. Trainin, I. Bar-Ya'akov, H. Borochov-Neori, et al., A pomegranate (Punica granatum L.) WD40-repeat gene is a functional homologue of Arabidopsis TTG1 and is involved in the regulation of anthocyanin biosynthesis during pomegranate fruit development, Planta 234 (2011) 865–881, https://doi.org/10.1007/s00425-011-1438-4.
[31] I.M. Zimmermann, M.A. Heim, B. Weisshaar, J.F. Uhrig, Comprehensive identification of Arabidopsis thaliana MYB transcription factors interacting with R/B-like BHLH proteins, Plant J. 40 (2004) 22–34, https://doi.org/10.1111/j.1365-313X.2004.02183.x.
[32] R. Stracke, M. Werber, B. Weisshaar, The R2R3-MYB gene family in Arabidopsis thaliana, Curr. Opin. Plant Biol. 4 (2001) 447–456, https://doi.org/10.1016/S1369-5266(00)00199-0.
[33] C. Dubos, R. Stracke, E. Grotewold, B. Weisshaar, C. Martin, L. Lepiniec, MYB transcription factors in Arabidopsis, Trends Plant Sci. 15 (2010) 573–581, https://doi.org/10.1016/j.tplants.2010.06.005.
[34] H. Jin, E. Cominelli, P. Bailey, A. Parr, F. Mehrtens, J. Jones, et al., Transcriptional repression by AtMYB4 controls production of UV-protecting sunscreens in Arabidopsis, EMBO J. 19 (2000) 6150–6161, https://doi.org/10.1093/emboj/19.22.6150.
[35] L. Lepiniec, I. Debeaujon, J.-M. Routaboul, A. Baudry, L. Pourcel, N. Nesi, et al., Genetics and biochemistry of seed flavonoids, Annu. Rev. Plant Biol. 57 (2006) 405–430, https://doi.org/10.1146/annurev.arplant.57.032905.105252.
[36] A. Gonzalez, M. Zhao, J.M. Leavitt, A.M. Lloyd, Regulation of the anthocyanin biosynthetic pathway by the TTG1/bHLH/Myb transcriptional complex in Arabidopsis seedlings, Plant J. 53 (2008) 814–827, https://doi.org/10.1111/j.1365-313X.2007.03373.x.
[37] K. Lin-Wang, K. Bolitho, K. Grafton, A. Kortstee, S. Karunairetnam, T.K. McGhie, et al., An R2R3 MYB transcription factor associated with regulation of the anthocyanin biosynthetic pathway in Rosaceae, BMC Plant Biol. 10 (2010) 50, https://doi.org/10.1186/1471-2229-10-50.
[38] R. Stracke, H. Ishihara, G. Huep, A. Barsch, F. Mehrtens, K. Niehaus, et al., Differential regulation of closely related R2R3-MYB transcription factors controls flavonol accumulation in different parts of the Arabidopsis thaliana seedling, Plant J. 50 (2007) 660–677, https://doi.org/10.1111/j.1365-313X.2007.03078.x.
[39] E. Oh, H. Kang, S. Yamaguchi, J. Park, D. Lee, Y. Kamiya, et al., Genome-wide analysis of genes targeted by PHYTOCHROME INTERACTING FACTOR 3-LIKE5 during seed germination in Arabidopsis, Plant Cell 21 (2009) 403–419, https://doi.org/10.1105/tpc.108.064691.
[40] D. Vom Endt, J.W. Kijne, J. Memelink, Transcription factors controlling plant secondary metabolism: what regulates the regulators? Phytochemistry 61 (2002) 107–114, https://doi.org/10.1016/S0031-9422(02)00185-1.
[41] S. Afrin, M. Nuruzzaman, J. Zhu, Z. Luo, Combinatorial interactions of MYB and bHLH in flavonoid biosynthesis and their function in plants, J. Plant Biol. Res. 3 (2014) 65–77 (Accessed January 20, 2020), https://www.semanticscholar.org/paper/Combinatorial-interactions-of-MYB-and-bHLH-in-and-Afrin-Nuruzzaman/3dbb4320d158f2507d93814141797fffa70dd0ed.
[42] E. Butelli, L. Titta, M. Giorgio, H.P. Mock, A. Matros, S. Peterek, et al., Enrichment of tomato fruit with health-promoting anthocyanins by expression of select transcription factors, Nat. Biotechnol. 26 (2008) 1301–1308, https://doi.org/10.1038/nbt.1506.
[43] M.M. Goodin, D. Zaitlin, R.A. Naidu, S.A. Lommel, Nicotiana benthamiana: its history and future as a model for plant–pathogen interactions, Mol. Plant Microbe Interact. 21 (2008) 1015–1026, https://doi.org/10.1094/mpmi-21-8-1015.
[44] A. Bombarely, H.G. Rosli, J. Vrebalov, P. Moffett, L.A. Mueller, G.B. Martin, A draft genome sequence of Nicotiana benthamiana to enhance molecular plant-microbe biology research, Mol. Plant Microbe Interact. 25 (2012) 1523–1530, https://doi.org/10.1094/mpmi-06-12-0148-ta.
[45] N.S. Outchkourov, C.A. Carollo, V. Gomez-Roldan, R.C.H. de Vos, D. Bosch, R.D. Hall, et al., Control of anthocyanin and non-flavonoid compounds by anthocyanin-regulating MYB and bHLH transcription factors in Nicotiana benthamiana leaves, Front. Plant Sci. 5 (2014) 1–9, https://doi.org/10.3389/fpls.2014.00519.
[46] J. Sun, L.Z. Lin, P. Chen, Study of the mass spectrometric behaviors of anthocyanins in negative ionization mode and its applications for characterization of anthocyanins and non-anthocyanin polyphenols, Rapid Commun. Mass Spectrom. 26 (2012) 1123–1133, https://doi.org/10.1002/rcm.6209.
[47] A. Zarei, Z. Zamani, A. Mousavi, R. Fatahi, M.K. Alavijeh, B. Dehsara, S.A. Salami, An effective protocol for isolation of high-quality RNA from pomegranate seeds, AAJPSB - Global Science Books 6 (2012), pp. 32–37.
[48] F. Sievers, D.G. Higgins, Clustal Omega for making accurate alignments of many protein sequences, Protein Sci. 27 (2018) 135–145, https://doi.org/10.1002/pro.3290.
[49] S. Kumar, G. Stecher, M. Li, C. Knyaz, K. Tamura, MEGA X: molecular evolutionary genetics analysis across computing platforms, Mol. Biol. Evol. 35 (2018) 1547–1549, https://doi.org/10.1093/molbev/msy096.
[50] T.L. Bailey, M. Boden, F.A. Buske, M. Frith, C.E. Grant, L. Clementi, et al., MEME suite: tools for motif discovery and searching, Nucleic Acids Res. 37 (2009) W202–W208, https://doi.org/10.1093/nar/gkp335.
[51] A. Untergasser, I. Cutcutache, T. Koressaar, J. Ye, B.C. Faircloth, M. Remm, et al., Primer3-new capabilities and interfaces, Nucleic Acids Res. 40 (2012) e115, https://doi.org/10.1093/nar/gks596.
[52] Z. Ben-Simhon, S. Judeinstein, T. Trainin, R. Harel-Beja, I. Bar-Yaakov, H. Borochov-Neori, et al., A "white" anthocyanin-less pomegranate (Punica granatum L.) caused by an insertion in the coding region of the leucoanthocyanidin dioxygenase (LDOX; ANS) gene, PLoS One 10 (2015) 1–21, https://doi.org/10.1371/journal.pone.0142777.
[53] M.W. Pfaffl, A new mathematical model for relative quantification in real-time RT-PCR, Nucleic Acids Res. 29 (2001), https://doi.org/10.1093/nar/29.9.e45 45e–45.
[54] T.W.J.M. van Herpen, K. Cankar, M. Nogueira, D. Bosch, H.J. Bouwmeester, J. Beekwilder, Nicotiana benthamiana as a production platform for artemisinin precursors, PLoS One 5 (2010) e14222, , https://doi.org/10.1371/journal.pone.0014222.
[55] N.S. Outchkourov, C.A. Carollo, V. Gomez-Roldan, R.C.H. de Vos, D. Bosch, R.D. Hall, et al., Control of anthocyanin and non-flavonoid compounds by anthocyanin-regulating MYB and bHLH transcription factors in Nicotiana benthamiana leaves, Front. Plant Sci. 5 (2014) 1–9, https://doi.org/10.3389/fpls.2014.00519.
[56] G.R. Lazo, P.A. Stein, R.A. Ludwig, A DNA transformation–competent arabidopsis genomic library in agrobacterium, Bio/Technology 9 (1991) 963–967, https://doi.org/10.1038/nbt1091-963.

[57] R.C.H. De Vos, S. Moco, A. Lommen, J.J.B. Keurentjes, R.J. Bino, R.D. Hall, Untargeted large-scale plant metabolomics using liquid chromatography coupled to mass spectrometry, Nat. Protoc. 2 (2007) 778–791, https://doi.org/10.1038/nprot.2007.95.

[58] A. Lommen, Metalign: interface-driven, versatile metabolomics tool for hyphenated full-scan mass spectrometry data preprocessing, Anal. Chem. 81 (2009) 3079–3086, https://doi.org/10.1021/ac900036d.

[59] Y.M. Tikunov, S. Laptenok, R.D. Hall, A. Bovy, R.C.H. de Vos, MSClust: a tool for unsupervised mass spectra extraction of chromatography-mass spectrometry ion-wise aligned data, Metabolomics 8 (2012) 714–718, https://doi.org/10.1007/s11306-011-0368-2.

[60] A. Mouradov, G. Spangenberg, Flavonoids: a metabolic network mediating plants adaptation to their real estate, Front. Plant Sci. 5 (2014) 1–16, https://doi.org/10.3389/fpls.2014.00620.

[61] A. Spinardi, G. Cola, C.S. Gardana, I. Mignani, Variation of anthocyanin content and profile throughout fruit development and ripening of highbush blueberry cultivars grown at two different altitudes, Front. Plant Sci. 10 (2019) 1045, https://doi.org/10.3389/fpls.2019.01045.

[62] L. Han, Z. Yuan, L. Feng, Y. Yin, Changes in the composition and contents of pomegranate polyphenols during fruit development, Acta Hortic. (2015) 53–61, https://doi.org/10.17660/actahortic.2015.1089.5.

[63] A.M. Gómez-Caravaca, V. Verardo, M. Toselli, A. Segura-Carretero, A. Fernández-Gutiérrez, M.F. Caboni, Determination of the major phenolic compounds in pomegranate juices by HPLC-DAD-ESI-MS, J. Agric. Food Chem. 61 (2013) 5328–5337, https://doi.org/10.1021/jf400684n.

[64] C.T. Payne, F. Zhang, A.M. Lloyd, GL3 encodes a bHLH protein that regulates trichome development in arabidopsis through interaction with GL1 and TTG1, Genetics 156 (2000) 1349–1362 http://www.genetics.org/content/156/3/1349.abstract.

[65] K. Lin-Wang, K. Bolitho, K. Grafton, A. Kortstee, S. Karunairetnam, T.K. McGhie, et al., An R2R3 MYB transcription factor associated with regulation of the anthocyanin biosynthetic pathway in Rosaceae, BMC Plant Biol. 10 (2010) 50, https://doi.org/10.1186/1471-2229-10-50.

[66] C. Dubos, J. Le Gourrierec, A. Baudry, G. Huep, E. Lanet, I. Debeaujon, et al., MYBL2 is a new regulator of flavonoid biosynthesis in Arabidopsis thaliana, Plant J. 55 (2008) 940–953, https://doi.org/10.1111/j.1365-313X.2008.03564.x.

[67] Z.S. Xu, K. Feng, F. Que, F. Wang, A.S. Xiong, A MYB transcription factor, DcMYB6, is involved in regulating anthocyanin biosynthesis in purple carrot taproots, Sci. Rep. 7 (2017) 45324, https://doi.org/10.1038/srep45324.

[68] T.A. Colquhoun, J.Y. Kim, A.E. Wedde, L.A. Levin, K.C. Schmitt, R.C. Schuurink, et al., PhMYB4 fine-tunes the floral volatile signature of Petunia × hybrida through PhC4H, J. Exp. Bot. 62 (2011) 1133–1143, https://doi.org/10.1093/jxb/erq342.

[69] H. Zhou, K. Lin-Wang, L. Liao, C. Gu, Z. Lu, A.C. Allan, et al., Peach MYB7 activates transcription of the proanthocyanidin pathway gene encoding leucoanthocyanidin reductase, but not anthocyanidin reductase, Front. Plant Sci. 6 (2015) 908, https://doi.org/10.3389/fpls.2015.00908.

[70] J. Bogs, F.W. Jaffé, A.M. Takos, A.R. Walker, S.P. Robinson, The grapevine transcription factor VvMYBPA1 regulates proanthocyanidin synthesis during fruit development, Plant Physiol. 143 (2007) 1347–1361, https://doi.org/10.1104/pp.106.093203.

[71] L. Deluc, J. Bogs, A.R. Walker, T. Ferrier, A. Decendit, J.M. Merillon, et al., The transcription factor VvMYB5b contributes to the regulation of anthocyanin and proanthocyanidin biosynthesis in developing grape berries, Plant Physiol. 147 (2008) 2041–2053, https://doi.org/10.1104/pp.108.118919.

[72] A. Gesell, K. Yoshida, L.T. Tran, C.P. Constabel, Characterization of an apple TT2-type R2R3 MYB transcription factor functionally similar to the poplar proanthocyanidin regulator PtMYB134, Planta 240 (2014) 497–511, https://doi.org/10.1007/s00425-014-2098-y.

[73] X.H. An, Y. Tian, K.Q. Chen, X.J. Liu, D.D. Liu, X. Bin Xie, et al., MdMYB9 and MdMYB11 are involved in the regulation of the ja-induced biosynthesis of anthocyanin and proanthocyanidin in apples, Plant Cell Physiol. 56 (2015) 650–662, https://doi.org/10.1093/pcp/pcu205.

[74] J.G. Schaart, C. Dubos, I. Romero De La Fuente, A.M.M.L. van Houwelingen, R.C.H. de Vos, H.H. Jonker, et al., Identification and characterization of MYB-bHLH-WD40 regulatory complexes controlling proanthocyanidin biosynthesis in strawberry (Fragaria × ananassa) fruits, New Phytol. 197 (2013) 454–467, https://doi.org/10.1111/nph.12017.

[75] M.A. Rahim, N. Busatto, L. Trainotti, Regulation of anthocyanin biosynthesis in peach fruits, Planta 240 (2014) 913–929, https://doi.org/10.1007/s00425-014-2078-2.

[76] N. Nesi, I. Debeaujon, C. Jond, G. Pelletier, M. Caboche, L. Lepiniec, The TT8 gene encodes a basic helix-loop-helix domain protein required for expression of DFR and BAN genes in Arabidopsis siliques, Plant Cell 12 (2000) 1863–1878, https://doi.org/10.1105/tpc.12.10.1863.

[77] C. Seitz, S. Ameres, K. Schlangen, G. Forkmann, H. Halbwirth, Multiple evolution of flavonoid 3′,5′-hydroxylase, Planta 242 (2015) 561–573, https://doi.org/10.1007/s00425-015-2293-5.

[78] R.L. Prior, X. Wu, Anthocyanins: structural characteristics that result in unique metabolic patterns and biological activities, Free Radic. Res. 40 (2006) 1014–1028, https://doi.org/10.1080/10715760600758522.

[79] X.C. Wen, J. Han, X.P. Leng, R.J. Ma, W.B. Jiang, J.G. Fang, Cloning and expression of UDP-glucose: flavonoid 3-O-glucosyltransferase gene in peach flowers, Genet. Mol. Res. 13 (2014) 10067–10075, https://doi.org/10.4238/2014.December.4.1.